ACS Catalysis

Research Article

pubs.acs.org/acscatalysis

Exo/*endo* Selectivity of the Ring-Closing Enyne Methathesis Catalyzed by Second Generation Ru-Based Catalysts. Influence of Reactant Substituents

Francisco Nuñez-Zarur, Xavier Solans-Monfort,* Luis Rodríguez-Santiago, and Mariona Sodupe

Departament de Química, Universitat Autònoma de Barcelona, Edifici Cn, 08193 Bellaterra, Spain

Supporting Information

ABSTRACT: The influence of enyne substituents in the product selectivity of the Ring-Closing Enyne Methathesis (RCEYM) catalyzed by the most common mesithyl-containing second-generation Ru-based Grubbs type complexes has been studied by means of density functional theory (DFT, B3LYP-D) calculations. For this, we have computed the energetics of the three proposed mechanism (*ene-then-yne*; *exo-yne-then-ene*, and *endo-yne-then-ene*) of a series of 11 different enynes that share the 1-allyloxyprop-2-yne skeleton. Three different substitutions have been taken into account: the alkyne fragment terminal position, the propargylic carbon, and the internal carbon of the alkene fragment. For the first two substitution positions, models including hypothetical electron-donor and electron-withdrawing substituents have been considered. Present calculations show that nonproductive pathways leading to catalyst deactivation are competitive with the catalytic cycle when nonsubstituted enynes are made to react. Nevertheless, these nonproductive pathways are prevented by the addition of small substituents in the alkene moiety and in the terminal position of the alkyne. In these cases, a methyl group in the alkene moiety prevents to a large extent the *ene-then-yne* route, and thus, the reaction preferentially proceeds through the *yne-then-ene* mechanism. This leads to the potential formation of both the *exo* and the *endo* products. Moreover, when the *ene-then-yne* route is prevented, the preference for one or the other product seems to depend on not only the steric hindrance of the substituents. In this way, enynes with terminal alkyne fragments proceed preferentially through the *exo* route. However, when the alkyne is internal, the two carbons of the alkyne fragment have similar atomic charges, and the two routes become competitive. Therefore, both *exo*- and *endo*- products can be formed, as seen experimentally.

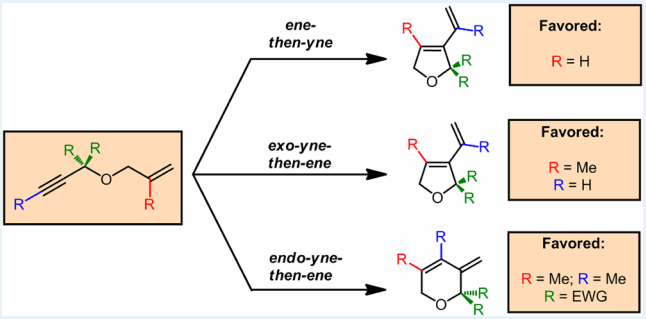

KEYWORDS: *homogeneous catalysis, enyne metathesis, N-heterocyclic carbene, DFT calculations, RCEYM, reaction mechanism*

INTRODUCTION

The enyne metathesis reaction[1−3] is a derivative process of the well-known alkene metathesis reaction (Scheme 1a).[4−9] In its intramolecular version, it consists in the skeletal reorganization of one alkene and one alkyne fragment leading to the formation of a cyclic conjugated 1,3-diene as shown in Scheme 1b.[2,10] This reaction is considered a very powerful tool in organic synthesis.[11−14] It allows the atom economical formation of cyclic functionalized products, usually present in many drugs and natural products. The reaction requires the presence of a catalyst to occur.[3,15] Several different complexes have been shown to catalyze the process, and among them, the newest generations of Mo-[16−18] and Ru-based[2,19,20] catalysts (Scheme 2a) are the most commonly used today. It is nowadays well accepted that complexes shown in Scheme 2a are not the real catalysts but precursors of the active species, which are obtained after the reaction of the precursor with one reactant molecule.[21−26] In the case of the enynes, the activation process can generate **1E** and **1Y** (Scheme 2b), which are supposed to be the active carbenes.[27] It is noteworthy that **1E** and **1Y** are the only considered species in this work, and thus, neither the

Scheme 1

a)

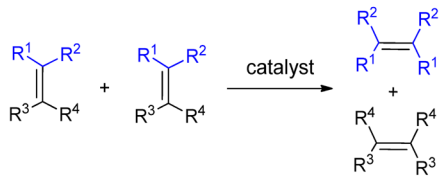

b)

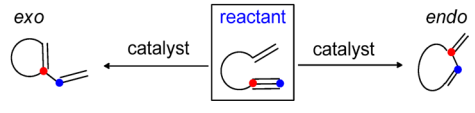

Received: September 4, 2012
Revised: December 17, 2012
Published: December 28, 2012

Scheme 2

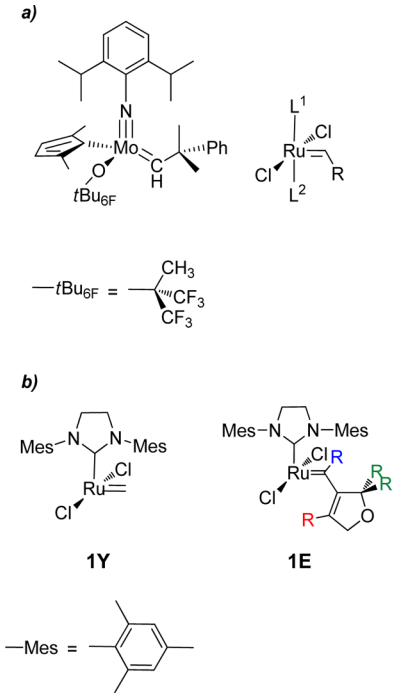

role of the precursor activation nor that of other L^1 (Scheme 2a) ligands has been taken into account in the present contribution.

Two different mechanisms have been proposed for both Mo- and Ru-based catalyzed processes: the *ene-then-yne* and the *yne-then-ene* pathways (Scheme 3 and 4).[13,17,27−33] They differ in the order in which the unsaturated fragments react with the catalyst, and the two can apply during both the precursor activation and the catalytic cycle. In particular, the activation process of the most common second-generation Ru-based precursors by the reaction with a model enyne (**a** in Scheme 5) through the *ene-then-yne* mechanism leads to the formation of complex **1Ea** (Scheme 3), whereas the activation process through an *yne-then-ene* mechanism generates **1Y** as the active species (Scheme 3).

Regarding the catalytic cycle, it has been suggested that the *yne-then-ene* pathway can proceed through two different routes: the *exo-yne-then-ene* (Scheme 3 and Scheme 4) and the *endo-yne-then-ene* one (Scheme 3 and Scheme 4).[13,29,31,32,34] The *exo* and *endo* designation refers to the position of the cleaved triple bond of the enyne in the final cyclic structure, the *exo* prefix indicating an exocyclic position of the triple bond (left site of Scheme 1b), whereas the *endo* one indicates that the cleaved triple bond is part of the ring structure (right site of Scheme 1b). Consequently, the *yne-then-ene* route can potentially lead to two distinct products,[29,32,34] and their formation arises from the different relative orientation between the reactant and the catalyst in the initial steps of the reaction. The product obtained from the reaction of 1-allyloxyprop-2-yne through the *exo-yne-then-ene* pathway is the 5-membered ring shown in Scheme 4b, and the one formed from the *endo-yne-then-ene* mechanism is the 6-membered ring shown in Scheme 4c. For

Scheme 3

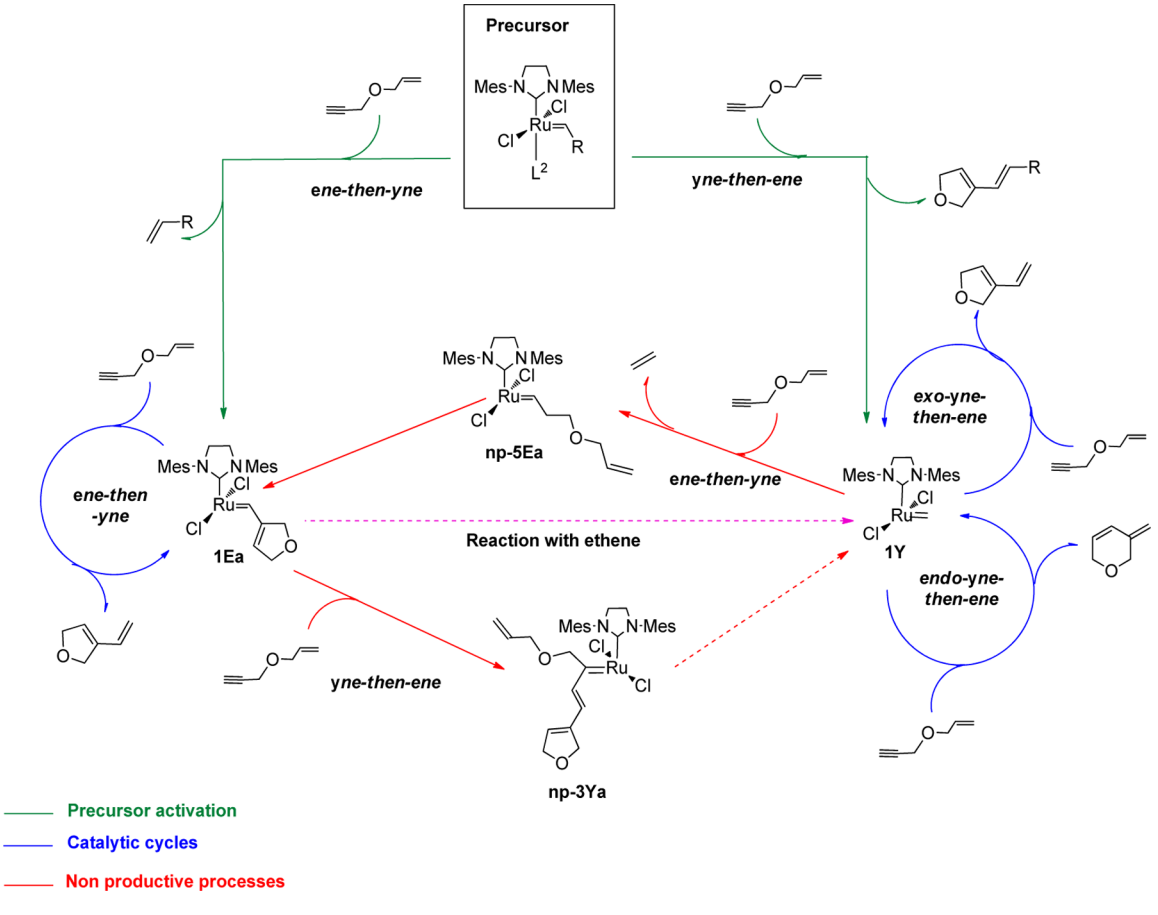

dx.doi.org/10.1021/cs300580g | ACS Catal. 2013, 3, 206−218

Scheme 4

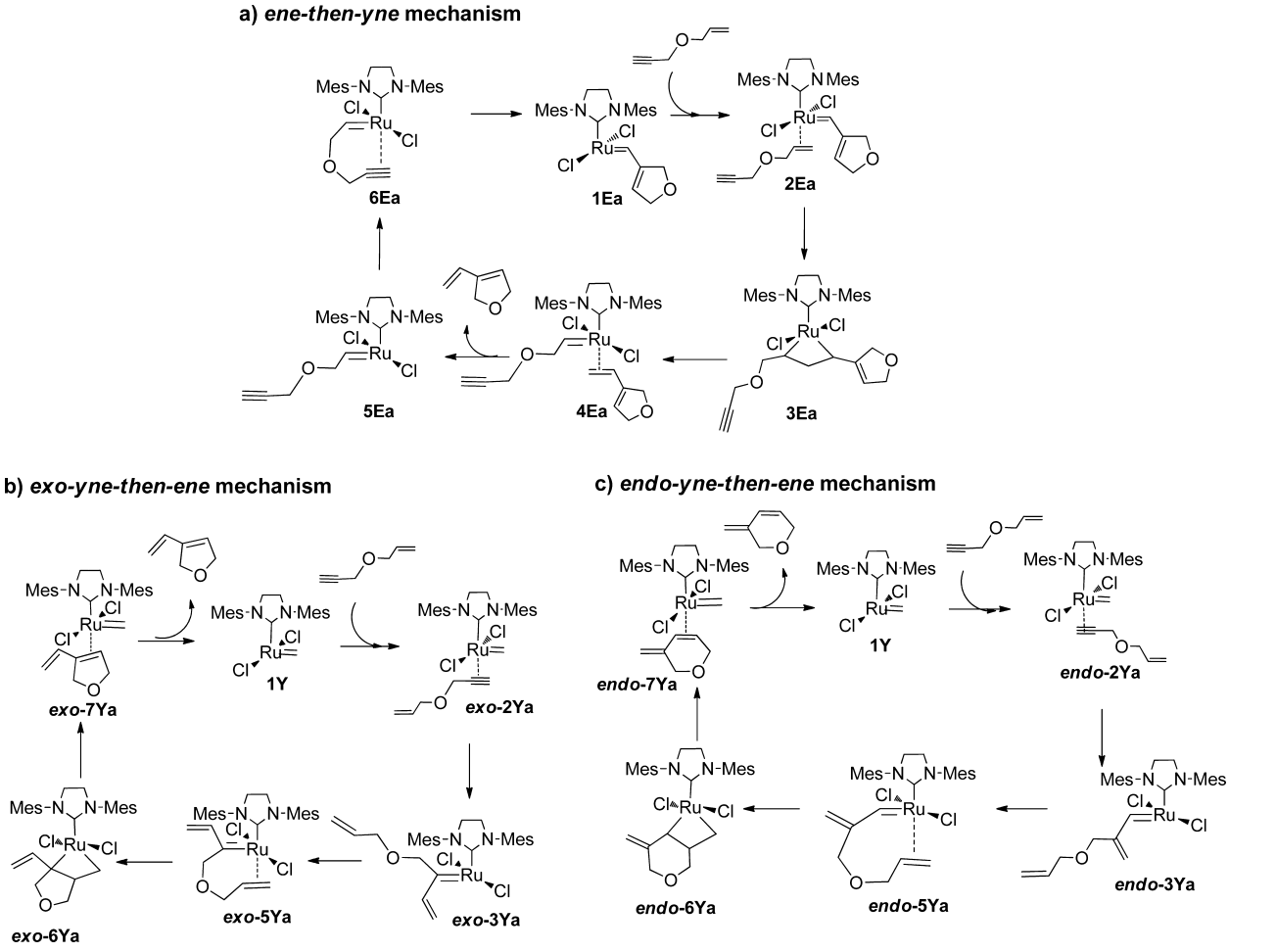

the *ene-then-yne* route, the reaction proceeds only through the *exo* approach,[32] as the bicyclic metallacycle arising from the *endo* orientation is too constrained to take place.

The situation is even more complex as other nonproductive processes can occur. Some of these processes originate from the fact that **1E** and **1Y** can also react first with the unsaturated fragment that is not involved in the catalytic cycle, and this is illustrated with the red arrows in Scheme 3. In particular, the reaction of **1Y** with the alkene fragment of the enyne **a** leads to the formation of **1Ea** in a process that has been shown to be very exergonic.[35] On the other hand, the reaction of **1Ea** with the alkyne moiety of the enyne **a** leads to a carbene containing two enyne molecules that according to the very recent MALDI-TOF experiments of Fogg and co-workers can be the origin of catalyst deactivation.[27] Finally, the addition of ethene in the media (Mori's conditions) favors the formation of **1Y**.[27]

For Ru-based complexes, most of the experimental data suggest that the *ene-then-yne* mechanism is the most probable one taking place.[27,28,30] Nevertheless, experiments presenting evidence in favor of the *yne-then-ene* also exist, and thus, none of them should be excluded a priori.[34,36] In fact, the nature of the predominant mechanism seems to depend on the catalyst, reactants, and reacting conditions,[29,32,34] and in particular, the substituents in the reacting enyne seem to have a significant effect.[27,29,32,34,37] Indeed, those reactants in which the alkene is sterically hindered and the alkyne fragment is internal provide significant amounts of the *endo* product.[29,32,34]

To the best of our knowledge, within all theoretical studies on the alkene metathesis reaction and its derivative processes,[38−59] very few works have focused on the ring-closing enyne metathesis,[35,37,60,61] and none of them has considered substituted enynes. Previous works on the RCEYM reaction concluded that subtle energy differences exist among the three postulated pathways, the *ene-then-yne* being usually slightly preferred.[37,60] In particular, in our recent theoretical work on the enyne metathesis reaction of the unsubstituted 1-allyloxyprop-2-yne (**a** in Scheme 5) with the Ru-based second-generation Grubbs−Hoveyda catalyst, we concluded that there is no clear intrinsic preference for either the *ene-then-yne* or the *yne-then-ene* mechanisms.[35] Moreover, when comparing the *exo-yne-then-ene* and the *endo-yne-then-ene* pathways, the former is energetically favored, and thus, the *exo* product would be the major one. Nevertheless, since the energy differences among the three potential catalytic mechanisms are small, we decided to perform a deeper study considering several enynes bearing small substituents close to the alkene and alkyne unsaturated fragments (**b**−**k** in Scheme 5).

The aim of this work is to analyze how substituents in the reactant may influence the *exo-*/*endo-* selectivity and explore which are the main factors in determining this selectivity. Efforts are mainly centered in the three catalytic cycles (*ene-then-yne*, *exo-yne-then-ene*, and *endo-yne-then-ene*), assuming that they are independent processes. In a second step, we explore the nonproductive routes arising from the reaction of **1E** or **1Y**

dx.doi.org/10.1021/cs300580g | ACS Catal. 2013, 3, 206−218

Scheme 5

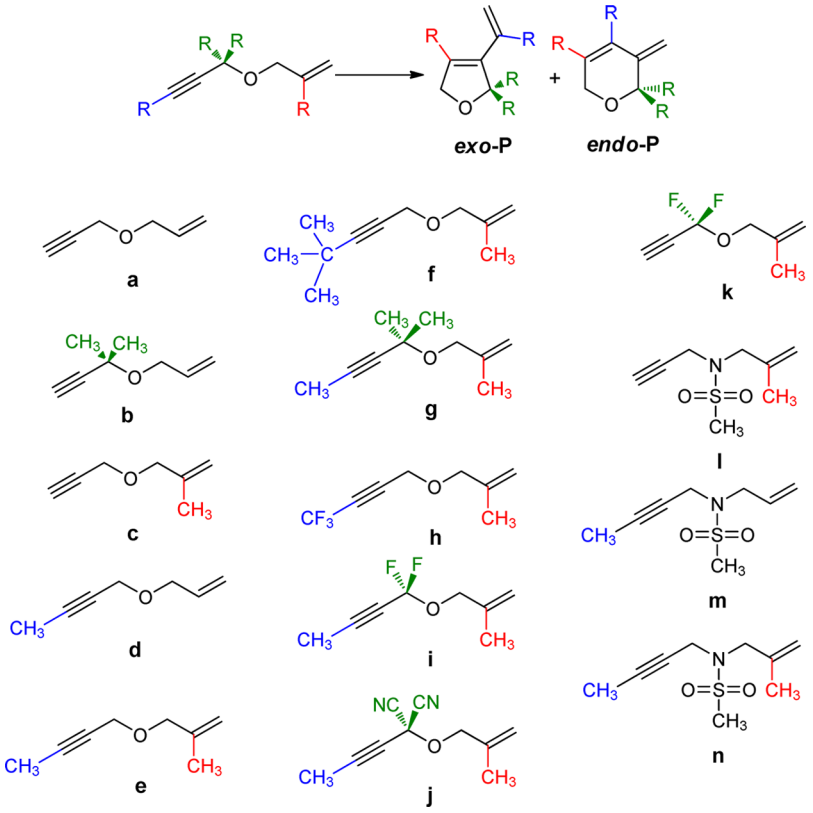

with the unsaturated fragment of the enyne that does not lead to the product formation, and we analyze how reactant substituents may influence these processes, too. We have only considered catalysts bearing mesityl N-substitutents as they are the most common ones in RCEYM reaction.[20,27,29,32,34,62] We have not taken into account the potential influence of the activation process as well as other side reactions in the reactivity and product selectivity. Consequently, we do not aim to understand the overall catalyst performances, but rationalize the factors that can influence the *exo-/endo-* selectivity. Comparison with the available experimental data in the literature shows that although the small energy differences found among the three catalytic cycles, the calculations reproduce reasonably well the experimental trends, and this allows us to conclude that the presence of substituents in the enyne skeleton is relevant on the *exo-/endo-* selectivity as well as their general reactivity in RCEYM reactions with Ru-based catalysts.

COMPUTATIONAL DETAILS

The methodology used in the present study is essentially equal to that used in our previous works on Ru-based alkene and enyne ring-closing metathesis.[35,56,63] All calculations have been performed with the B3LYP[64,65] hybrid density functional as implemented in Gaussian03.[66] The optimized geometries have been obtained representing ruthenium with the quasi-relativistic effective core pseudopotentials (RECP) of the Stuttgart−Bonn group and the associated basis sets augmented with a polarization function,[67,68] and all other atoms with a 6-31G(d,p) basis set[69,70] (BSA). The nature of all intermediates and transition structures have been verified by vibrational analysis. Energies are obtained from single point calculations, at the BSA optimized geometries, with a larger basis including diffuse functions for C, N, O, F, H, and Cl, 6-31++G(d,p) and the same RECP for ruthenium (BSB).[71] The gas phase thermal corrections are evaluated at 298.15 K and 1 atm using BSA. Solvent effects have been included by performing single point calculations with the Gaussian03 package at the gas phase optimized geometries using the C-PCM continuum model[72−74] and a cavity generated using the United Atom Topological Model on radii optimized at the HF/6-31G(d) level of theory.[75] The experimentally frequently used CH_2Cl_2 has been chosen as solvent. These conditions (solvent, pressure, and temperature) are close to those used in the experiments that inspired the present work[20,62] and quite common in metathesis reactions. Moreover, since dispersion forces have been shown to be important in the alkene metathesis reaction,[25,47,76,77] they have been taken into account, including Grimme's empirical correction at the optimized geometry ($D = -S_6 \sum_{i=1}^{Nat-1} \sum_{j=i+1}^{Nat} (C_6^{ij}/R_{ij}^6) f_{dmp}(R_{ij})$; $S_6 = 1.05$ as established for the B3LYP functional)[78,79] with the MOLDRAW program.[80] It is noteworthy that our previous work on the Grubbs−Hoveyda type precursors activation shows that B3LYP-D provides values in good agreement with those obtained with the more recently developed M06L functional,[63] which has been shown to properly describe the olefin metathesis reaction.[25,47,76,77]

The effect of further enlarging the basis sets in some key transition structures has been evaluated by performing B3LYP/BSC optimizations, in which the BSC basis set includes the same representation used before for ruthenium and the 6-311+G(d,p) basis set for the remaining elements. The energy barriers with respect to separated reactants vary only by about 2−3 kcal mol^{-1}, but more importantly, main trends are conserved (see Supporting Information, Figure S1 and Table S1 for further details).

dx.doi.org/10.1021/cs300580g | ACS Catal. 2013, 3, 206−218

Table 1. Comparison between the Computed Gibbs Energy Barriers for the Alkyne Skeletal Reorganization and the Gibbs Energy Barrier Relationship Derived from the Reported Experimental Yields (Refs 29 and 32)[a]

	exp. ratio					
reactant	*exo*-	*endo*-	$\Delta\Delta G^{\ddagger}_{exp}$ [b]	$\Delta G^{\ddagger}_{exo}$	$\Delta G^{\ddagger}_{endo}$	$\Delta\Delta G^{\ddagger}_{comput}$ [b]
l	100%	not obs.	>2.7	+7.5	+10.8	+3.3
m	87%	7%	+1.5	+13.9	+12.9	−1.0
n	50%	50%	0.0	+11.6	+9.4	−2.2

[a]Energies in kcal mol^{-1}. [b]$\Delta\Delta G^{\ddagger}_{comput} = \Delta G^{\ddagger}_{endo} - \Delta G^{\ddagger}_{exo}$.

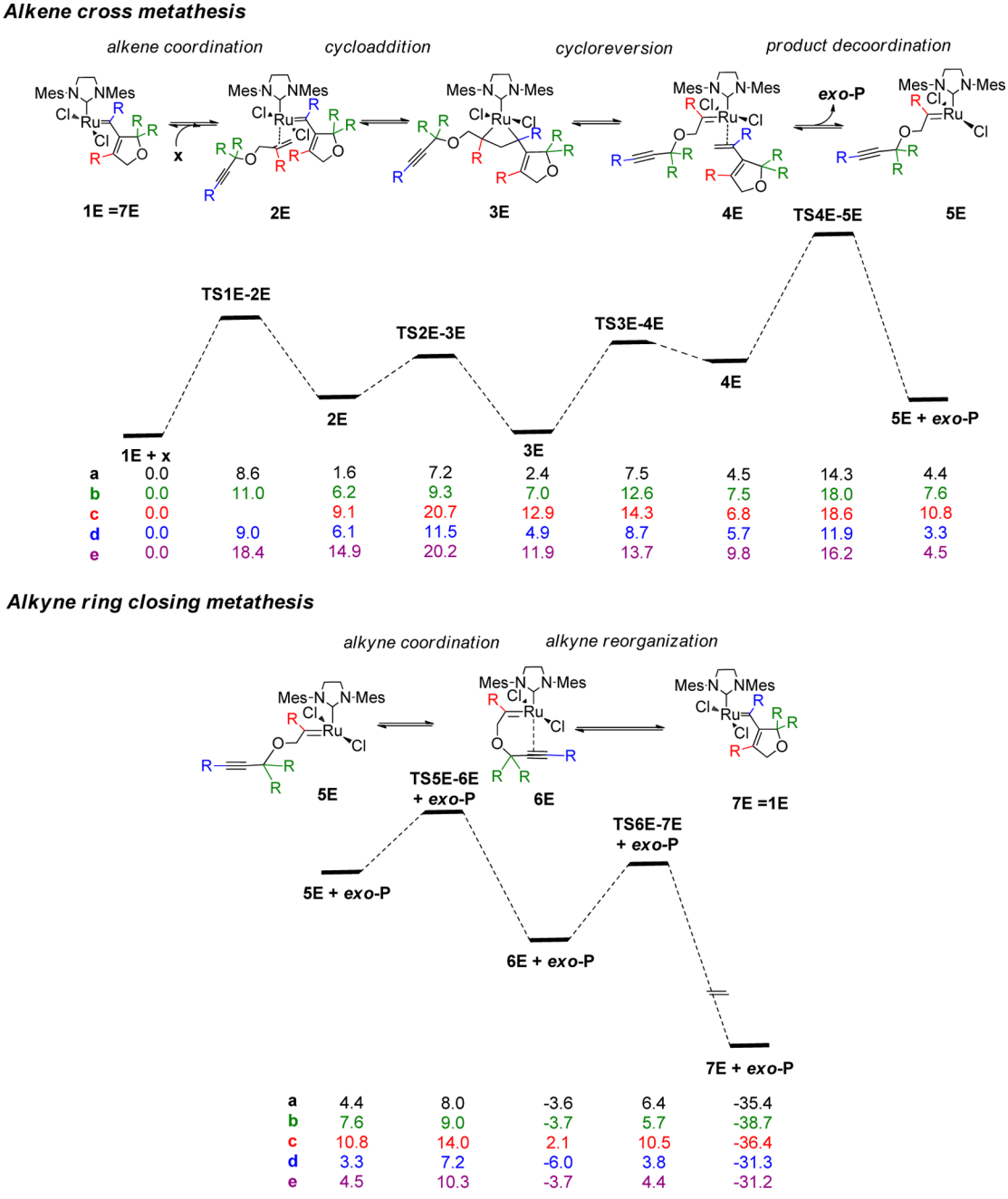

Figure 1. Free energy profile ($G + \Delta G_{solv} + D$) for the RCEYM catalytic cycle of enynes **a**−**e** through the *ene-then-yne* pathway. All values are in kcal mol^{-1}. See Scheme 5 for reactants' definitions.

The energetics reported in the manuscript ($G_{gp} + \Delta G_{solv} + D$) are based on gas phase Gibbs energies (G_{gp}) plus solvation free energies (ΔG_{solv}) and Grimme's correction for dispersion forces (D). Primary data as well as relative energies based on G_{gp} and $E_{gp} + \Delta G_{solv}$ can be found in the Supporting Information.

To evaluate the accuracy of our calculations, we took three model enynes (**l**−**n** in Scheme 5) of complexes whose *exo*-/

dx.doi.org/10.1021/cs300580g | *ACS Catal.* 2013, 3, 206−218

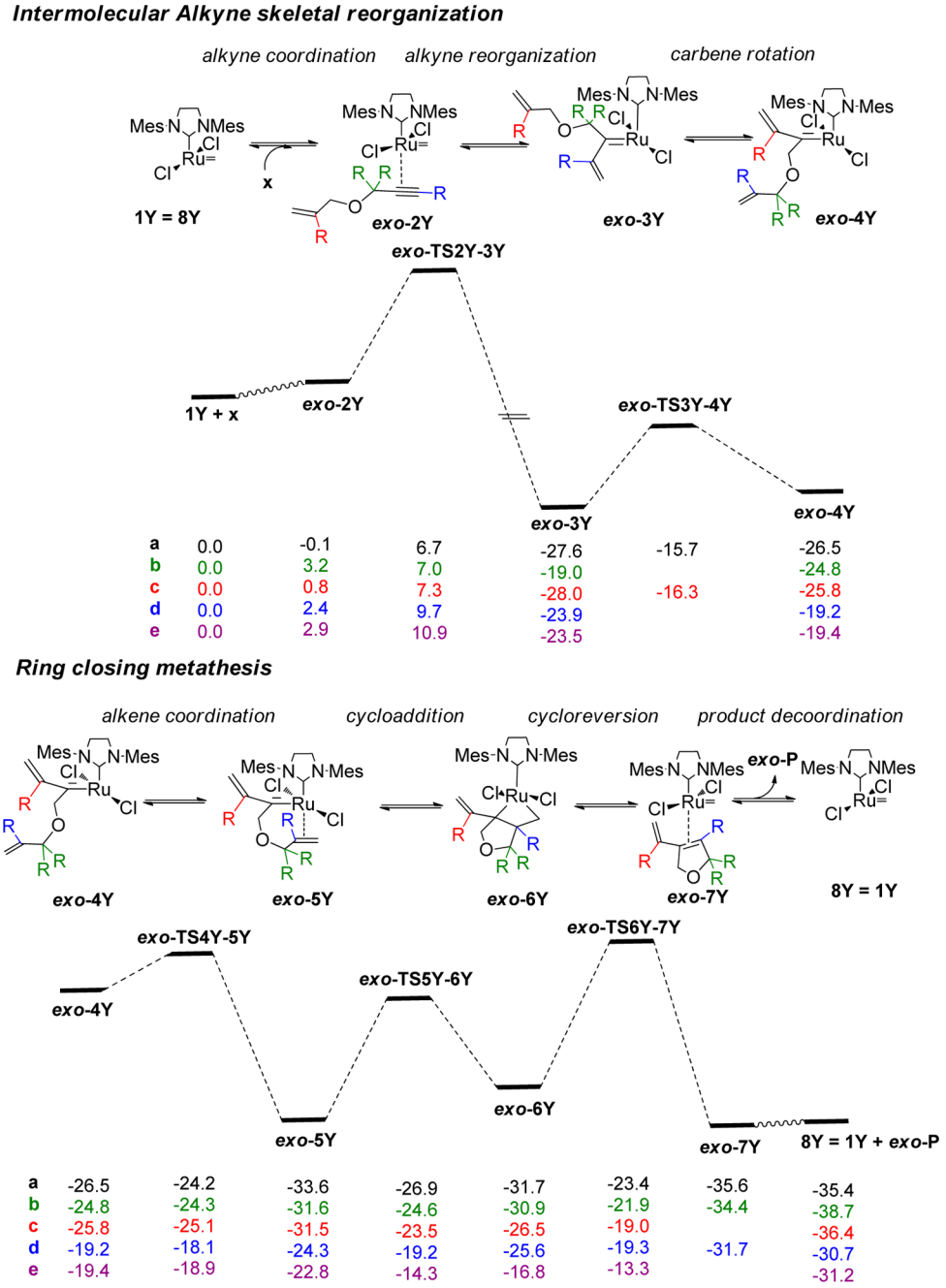

Figure 2. Free energy profile ($G + \Delta G_{solv} + D$) for the RCEYM catalytic cycle of enynes **a**–**e** through the *exo-yne-then-ene* pathway. All values are in kcal mol^{-1}. See Scheme 5 for reactants' definitions.

endo- selectivity has been measured experimentally.[29,32] It is noteworthy that in our models, the tosylamine group has been simplified to methanesulfonamide to reduce the computational cost. For **l**, **m**, and **n** enynes, we computed the energetics of the determinant transition structures (see below), and we compared our calculations with the relative Gibbs energies that one can extrapolate from the *exo-*/*endo-* yields reported experimentally. Table 1 reports the calculated energetics and the experimentally derived *exo-*/*endo-* $\Delta\Delta G^{\ddagger}$ values. It is shown that the experimentally observed trends are well reproduced by the calculations, although theoretical values overestimate the feasibility of the *endo-yne-then-ene* route by about 2.5 kcal mol^{-1}. This may arise either from the limitations of the calculations or from the effect of other side reactions not considered. In particular, the reaction of **1Y** with the enyne through an *ene-then-yne* mechanism can form **1E** in a very exergonic process, and thus, this can favor the *ene-then-yne* route, leading to larger amounts of the *exo* product. The energetics of this side process are discussed below.

RESULTS AND DISCUSSION

The ring-closing enyne metathesis (RCEYM) reaction of different enynes enclosing the 1-allyloxyprop-2-yne skeleton (**a**–**k** in Scheme 5) was considered. For these species, the final product contains a 5-membered ring if the catalytic cycle from **1E** takes place through an *ene-then-yne* pathway or if the reaction from **1Y** occurs through an *exo-yne-then-ene* mechanism. Alternatively, a 6-membered ring is formed if the process

dx.doi.org/10.1021/cs300580g | ACS Catal. 2013, 3, 206–218

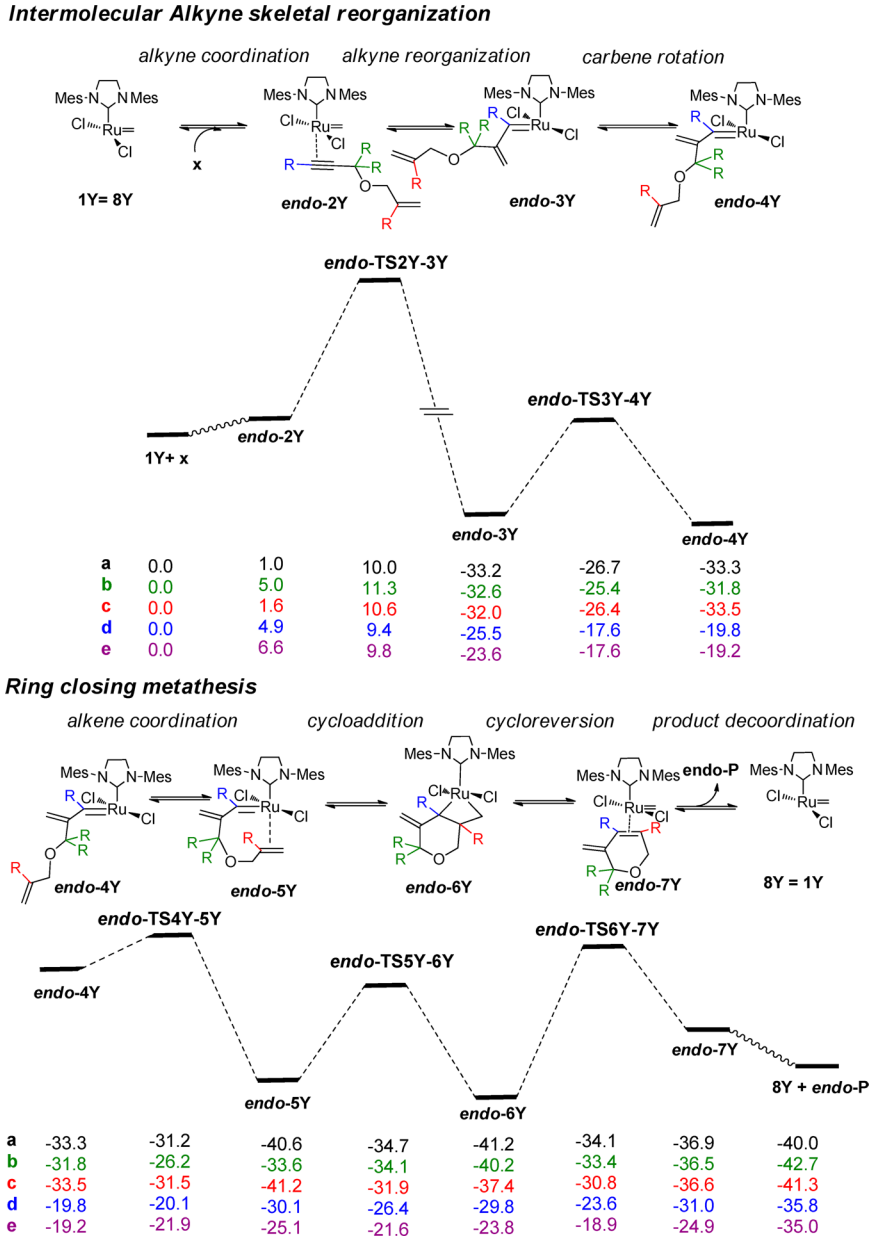

Figure 3. Free energy profile ($G + \Delta G_{solv} + D$) for the RCEYM catalytic cycle of enynes **a**−**e** through the *endo-yne-then-ene* pathway. All values are in kcal mol^{-1}. See Scheme 5 for reactants' definitions.

proceeds from **1Y** through the *endo-yne-then-ene* route (***exo*-P** and ***endo*-P** in Scheme 5). It is noteworthy that for five of these reactants (**a**−**e**), we considered the whole catalytic cycle of the three postulated reaction mechanisms (*ene-then-yne*, *exo-yne-then-ene*, and *endo-yne-then-ene*), and this will be discussed in the first part of the results and discussion section. In this part, results are presented assuming that both **1Y** to **1E** are present in the reaction mixture and proceed independently of their interconversion. In a second part, the nonproductive reactions of **1Y** and **1E** with the unsaturated fragment of the enyne that does not lead to products are also analyzed. These reactions lead to the formation of **1E** when **1Y** reacts with the alkene fragment of the enyne and to species that could favor the catalyst deactivation when **1E** reacts with the alkyne end as shown by Fogg and co-workers (red arrows in Scheme 3).[27] Therefore, they can have an important role in determining the amount of active carbene present in the reaction mixture and influence the final yields. Finally, in the last part, we will discuss reactants **f**−**k** (Scheme 5), for which we only considered the key elementary step (**TS2Y-3Y**) of the two different *yne-then-ene* catalytic cycles: the *exo* and *endo* orientations. Note that conclusions arising from this part would be more representative of reactions taking place in the presence of ethene. Nevertheless, according to our calculations, the *ene-then-yne* pathway is also significantly hindered for these species, even without the presence of ethene (vide infra).

The nomenclature used in the text is constructed from a set of a number and two letters. The number specifies the nature of the intermediate as defined in Scheme 4; the capital letter indicates if a specific intermediate is involved in an *ene-then-yne* (**E**) process or in an *yne-then-ene* (**Y**) one, and the lower case letter identifies the nature of the enyne (**a**−**k**). Transition structures are called adding **TS** before the two names of the interconnected intermediates. The words ***exo*** and ***endo*** are

dx.doi.org/10.1021/cs300580g | *ACS Catal.* 2013, 3, 206−218

added when needed to state the relative orientation between the incoming alkyne fragment and the active species. The transition structures and intermediates involved in the nonproductive processes are referred placing **np** before the number and the two letters.

Effect of Reactant Substituents in the Energetics of the Three Pathways. Figures 1−3 show the free energy profiles of the methyl-substituted reactants for the *ene-then-yne* (Figure 1), *exo-yne-then-ene* (Figure 2), and *endo-yne-then-ene* (Figure 3) pathways, and Table 2 summarizes the energy

Table 2. Nature of the Highest Transition Structure (TS) and the Global Gibbs Energy Barriers ($\Delta G^{\ddagger}$) in kcal mol^{-1} for the RCEYM Productive Catalytic Cycles of Enynes a−e[a]

	ene-then-yne		*exo-yne-then-ene*		*endo-yne-then-ene*	
reactant[b]	TS[c]	$\Delta G^{\ddagger}$	TS	$\Delta G^{\ddagger}$	TS	$\Delta G^{\ddagger}$
a	$TS_{4E\text{-}5E}$	+14.3	$TS_{2Y\text{-}3Y}$	+6.7	$TS_{2Y\text{-}3Y}$	+10.0
b	$TS_{4E\text{-}5E}$	+18.0	$TS_{2Y\text{-}3Y}$	+7.0	$TS_{2Y\text{-}3Y}$	+11.3
c	$TS_{2E\text{-}3E}$	+20.7	$TS_{2Y\text{-}3Y}$	+7.3	$TS_{2Y\text{-}3Y}$	+10.6
d	$TS_{1E\text{-}2E}$	+11.9	$TS_{2Y\text{-}3Y}$	+9.7	$TS_{2Y\text{-}3Y}$	+9.4
e	$TS_{2E\text{-}3E}$	+20.2	$TS_{2Y\text{-}3Y}$	+10.9	$TS_{2Y\text{-}3Y}$	+9.8

[a]These barriers are computed as the difference between separated reactants and the highest transition structure. [b]See Scheme 5 for reactants' definitions. [c]See Scheme 4 for structures' definitions.

difference between the reactants and the highest transition structure. The reader can find the optimized geometries of all stationary points (Supporting Information, Figures S2−S16) and their Cartesian coordinates in the Supporting Information.

The *ene-then-yne*, the *exo-yne-then-ene*, and the *endo-yne-then-ene* pathways for the reaction of enyne **a** were described in detail in our previous contribution.[35] The *ene-then-yne* mechanism (Figure 1) implies: (i) a cross metathesis process between **1Ea** and the alkene fragment of the enyne, thus forming the final product (top part of Figure 1), and (ii) the intramolecular alkyne fragment rearrangement that leads to the regeneration of the active species (bottom part of Figure 1). The cross-metathesis process implies four elementary steps: the enyne coordination, the cycloaddition, the cycloreversion, and the product release. All these steps are essentially isoergic (the highest intermediate lies at 4.5 kcal mol^{-1} above separated reactants) and imply low energy barriers (the highest value being 9.8 kcal mol^{-1} for an individual step). On the other hand, the alkyne skeletal reorganization is strongly exergonic, and it consists of two steps: the alkyne coordination and the reorganization itself. Interestingly, the two steps are again easily produced ($\Delta G^{\ddagger}$ for each step being lower than 10 kcal mol^{-1}), and since both steps are exergonic, this leads to transition structures that are lower in free energy than those of the cross-metathesis process.

The *exo-yne-then-ene* (Figure 2) and the *endo-yne-then-ene* (Figure 3) pathways imply steps similar to those taking place in the *ene-then-yne* route, but they occur in different order. In this way, the reaction between **a** and **1Y** starts with an intermolecular alkyne reorganization that leads to the formation of a conjugated carbene **3Ya** (top part of Figures 2 and 3). From **3Ya** carbene rotation takes place. This rotation forms **4Ya**, from which the coordination of the alkene fragment of the enyne occurs. This favors the ring-closing metathesis process that leads to the product release and the regeneration of the active **1Y** species (bottom part of Figures 2 and 3). As found in the *ene-then-yne* mechanism, the alkyne reorganization implies two steps (alkyne coordination and alkyne reorganization), and it is strongly exergonic. Moreover, it implies relatively low energy barriers and, although we could not locate the transition structure for the alkyne coordination, the **TS2Ya-TS3Ya** transition structure lies at only 6.7 and 10.0 kcal mol^{-1} above separated reactants for the *exo-* and *endo-* orientations, respectively. The ring-closing metathesis process involves four steps (alkene coordination, cycloaddition, cycloreversion, and product decoordination), and it is overall slightly exoergic (ΔG being −8.9 and −6.7 kcal mol^{-1} for the *exo-* and *endo-* orientations, respectively). The computed energy barriers are all low (the highest being 8.3 kcal mol^{-1}), and thus, all transition structures lie far below separated reactants, suggesting that once the alkyne skeletal reorganization has taken place, the process is irreversible.

In summary, for enyne **a**, present calculations suggest that the preferred pathway is the *exo-yne-then-ene* pathways, whose highest transition structure lies 6.7 kcal mol^{-1} above the separated reactants, followed by the *endo-yne-then-ene* route (highest transition structure being at 10.0 kcal mol^{-1}) and the *ene-then-yne* pathway ($\Delta G^{\ddagger}$ = 14.3 kcal mol^{-1}), as is summarized in Table 2.

As expected, the inclusion of substituents in the enynes does not alter the reaction mechanism of any of the three considered processes, and the number and nature of the elementary steps remains essentially the same. The optimized structures of all stationary points present the salient geometrical features described in our previous work,[35] and thus, they will not be discussed here. It is worth mentioning that for the *yne-then-ene* pathway, we have not been able to localize the transition structure associated with the initial alkyne coordination (**1Y** → *exo*/*endo*-**2Y**). In fact, all attempts to localize this saddle point failed, and the restricted potential energy surface explorations performed revealed a very flat region. Moreover, for enynes with substitutents at the alkene fragment or at the propargylic position, we have not been capable to localize the transition structures associated with the carbene rotation (***exo*-TS3Y-4Y**). In these cases, the larger distortion of the metal fragment because of steric repulsion with the chlorine ligands made this location more complex. Indeed, our potential energy explorations suggest that these transition structures would probably be slightly higher in energy than that for other enynes and may imply more than one step. Nevertheless, since **3Y** relative free energies with respect to separated reactants range between −27.6 and −19.0 kcal mol^{-1}, we expect that ***exo*-TS3Y-4Y** will have little influence in determining the *exo*/*endo* selectivity[35]

While the nature of the elementary steps is not affected by the presence of pending groups in the 1-allyloxyprop-2-yne skeleton, the energetics of the three potential reaction mechanisms vary significantly, depending on the reacting enyne substituents (Figures 1−3). The presence of two methyl substituents in the propargylic position (**b** in Scheme 5, green values in Figures 1−3) has the general effect of disfavoring the thermodynamics of the intermolecular alkene (**2Eb**) and alkyne (***exo*-2Yb** and ***endo*-2Yb**) coordination by about 3−5 kcal·mol^{-1}. In the particular cases of the *exo* and *endo-yne-then-ene* pathways, the effect is more pronounced for the *endo* approach and essentially is not transferred to the following elementary steps. As a consequence, the highest transition structures located are the ***exo*-TS2Yb-3Yb** and ***endo*-TS2Yb-3Yb** species, the energy barriers being 7.0 and 11.3 kcal mol^{-1} for the *exo-yne-then-ene* and *endo-yne-then-ene* routes, respec-

dx.doi.org/10.1021/cs300580g | ACS Catal. 2013, 3, 206−218

Table 3. Reaction Energies (ΔG) and Free Energy Differences between the Highest Transition Structure and Separated Reactants ($\Delta G^{\ddagger}$) for the 1Y to 1E Conversion and 1E to np-3Y Nonproductive Processes[a]

	1Y → 1E conversion				1E → np-3Y reaction		
reactant	$\Delta G_{1Y\text{-}npSE}$	$\Delta G_{1Y\text{-}1E}$	$\Delta G^{\ddagger}$	$\Delta G^{\ddagger}_{prod}$[b]	$\Delta G_{1E\text{-}np3Y}$	$\Delta G^{\ddagger}$	$\Delta G^{\ddagger}_{prod}$[c]
a	+1.4	−38.4	+9.1	+6.7	−25.7	+11.9	+14.3
b	+3.8	−42.5	+10.6	+7.0	−13.0	+14.5	+18.0
c	+7.3	−39.9	+14.2	+7.3	−21.4		+20.7
d	+3.7	−30.3		+9.4	−12.9	+19.4	+11.9
e	+7.0	−28.7		+9.8	−16.6		+20.2

[a]See Scheme 3 for structure labeling. [b]Highest in free energy transition structure of the *exo-yne-then-ene* catalytic cycle. [c]Highest in free energy transition structure of the *ene-then-yne* catalytic cycle.

tively. This shows that the presence of small substituents in the propargylic position does not alter the preference for the *exo-yne-then-ene* path. For the *ene-then-yne* mechanism, the effects of hindering the alkene coordination are transferred along the alkene cross metathesis process, since the transition structures associated with the subsequent cycloaddition, cycloreversion, and product release steps are higher in energy than the equivalent stationary points for the parent system **a**. The resulting free energy difference between the lowest intermediate and the highest transition structure, which arises from the difference between the initial reactants and the product decoordination transition structure (**TS4Eb-5Eb**), is 18.0 kcal mol^{-1}. Overall, present calculations suggest that the addition of relatively small substituents in the propargylic position of the enyne skeleton mainly disfavors the *ene-then-yne* pathway and the *endo-yne-then-ene* one.

The addition of a methyl group as a substituent at the alkene fragment (**c** in Scheme 5, red values in Figures 1−3) has very little influence on the alkyne skeletal reorganization. Note that the resulting energy barriers for the individual steps of the alkyne skeletal reorganization (***exo-*** and ***endo-TS2Yc-3Yc*** and **TS5Ec-6Ec**) differ by at most 1.6 kcal mol^{-1} with respect to those of the parent enyne **a**. In contrast, the effect on the alkene metathesis process is much more pronounced, and this is especially important in the cycloaddition and cycloreversion steps (**TS2Ec-3Ec**, **TS3Ec-4Ec**, **TS5Yc-6Yc**, and **TS6Yc-7Yc**). This applies to the three mechanisms as all intermediates and transition structures associated with the alkene metathesis process are generally disfavored, and they are usually higher in energy with respect to the reactants than the equivalent species for the reaction of **a**. As a consequence, the highest transition structure for the *ene-then-yne* route is no more the alkene dissociation but the cycloaddition (**TS2Ec-3Ec**). The free energy differences between reactants and the highest transition structure for the RCEYM of species **c** are 20.7 kcal mol^{-1} when proceeding through the *ene-then-yne* mechanism, 7.3 kcal mol^{-1} through the *exo-yne-then-ene* pathway, and 10.6 kcal mol^{-1} for the *endo-yne-then-ene* one. Thus, according to the calculations, the *ene-then-yne* route will be strongly hindered, and this result agrees with the already described difficulties to form tetrasubstituted olefins through Ru-based catalyzed olefin metathesis.[81−86]

The effects induced by the addition of a methyl group in the terminal position of the alkyne fragment (**d**, blue values in Figures 1−3) are mainly focused on the alkyne skeletal reorganization of the *yne-then-ene* pathways. In particular, although the alkyne coordination becomes more energetically demanding for both the *exo-* and the *endo-* orientations, this does not always correlate with a more disfavored alkyne skeletal reorganization. For instance, while the ***exo*-TS2Yd-3Yd** is about 3 kcal mol^{-1} higher than the equivalent process for the parent enyne **a**, the alkyne skeletal reorganization energy barrier of the *endo* approach marginally decreases (0.6 kcal mol^{-1}) (***endo*-TS2Yd-3Yd**). As a consequence, the two energy barriers become of similar height (9.7 vs 9.4 kcal mol^{-1}), and thus, the two orientations seem to be competitive. Overall, although the *ene-then-yne* pathway has slightly higher free energy barriers, the Gibbs energy differences between the initial reactants and the highest transition structure of the three processes are relatively similar. In any case, this is the first example in this work in which calculations suggest that the *endo* product could be obtained, and this partially agrees with the usual detection of this product in experiments with enyne substrates bearing an internal alkyne.[29,32,34]

Finally, we explored the reactivity of a disubstituted enyne having a methyl group in the terminal position of the alkyne moiety and another one in the alkene fragment (**e** in Scheme 5, purple values in Figures 1−3). The influence of the two substituents seems to be mainly additive: Similarly to what is obtained for **c**, enyne **e** presents a strongly disfavored *ene-then-yne* pathway as evidenced by the fact that the cycloaddition transition structure is 20.2 kcal mol^{-1} above separated reactants. Moreover, as **d**, the alkyne skeletal reorganization of **e** presents similar energetics for the *exo-yne-then-ene* and *endo-yne-then-ene* routes. Consequently, if all processes were independent, one would expect similar amounts of *exo* and *endo* products, the former obtained through the *exo-yne-then-ene* pathway exclusively.

Nonproductive Processes: 1Y to 1E Interconversion and Catalyst Deactivation. As already mentioned, other processes apart from the productive catalytic cycles can occur during the global process. In particular, **1Y** and **1E** can react with the unsaturated fragment of the enyne that does not lead to the desired products. The reaction of **1Y** with the alkene moiety leads to the formation of **1E**, while the reaction of **1E** with the alkyne moiety can lead to catalyst deactivation, as recent experiments of Fogg and co-workers have suggested (Scheme 3).[27]

In our previous study,[35] we considered the reaction of enyne **a** with **1Y** through an *ene-then-yne* mechanism as well as the reaction of **a** with **1Ea** through an *yne-then-ene* pathway. The reaction mechanism implies the same elementary steps as described above, and the unique difference is the nature of the carbene. Interestingly, the formation of **1Ea** by reaction of **1Y** with the alkene fragment of **a** is extremely exergonic because of the alkyne skeleton rearrangement, and it presents low energy barriers, the highest transition structure lying 9.1 kcal mol^{-1} above **1Y** + **a** (Table 3). This suggests that this process is competitive with the productive *exo-yne-then-ene* catalytic cycle ($\Delta G^{\ddagger}$ = 6.7 kcal mol^{-1}) and thus, since the former reaction is

dx.doi.org/10.1021/cs300580g | ACS Catal. 2013, 3, 206−218

highly exergonic and regeneration of **1Y** from **1Ea** does not seem plausible, this nonproductive process would increase the amount of **1Ea** in the reaction mixture. It is noteworthy that in the limit case that equilibrium would be reached, no **1Y** would be present in the reaction mixture.

On the other hand, the reaction of **1Ea** with the alkyne fragment of **a** is also a very exergonic process that leads to carbene species containing two enyne units (Scheme 3). The most energetically demanding process is the alkyne reorganization (**np-TS2Ya-3Ya**) whose transition structure lies only 11.9 kcal mol^{-1} above separated reactants. This value is slightly lower than that computed for the productive *ene-then-yne* catalytic cycle, and thus, it suggests that catalyst deactivation from **1Ea** can easily occur, leading to very small amounts of the final product. This was recently reported by Fogg and co-workers,[27] who showed that unsubstituted enynes lead to very small yields of final product and the formation of Ru complexes containing two enyne units.

We have also evaluated how the presence of substituents in the enyne modifies the thermodynamics of these two nonproductive processes. Moreover, for some selected cases, we have localized the highest in free energy transition structures assuming that the presence of bulkier groups will not change the nature of these species. The obtained results are summarized in Table 3. The computed trends are similar to those found for the productive processes. In particular, the addition of a methyl group in the alkene moiety (enyne **c**), disfavors the reaction of **1Y** with alkene fragment of the reacting enynes: formation of the intermediate carbene **np-5Ec** becomes significantly more endoergic, 7.3 kcal mol^{-1}, and the Gibbs energy difference between **1Y** + **c** and **np-TS4Ec-5Ec** increases to 14.2 kcal mol^{-1}, suggesting that the productive *yne-then-ene* pathways are the preferred process in this case. On the other hand, the presence of substituents in the alkyne moiety (enyne **b**, **d**, and **e**) has an effect on the reaction of **1E** with the alkyne fragment of the enyne. In general for these cases, the presence of substituents makes the reaction thermodynamically less favorable. Moreover, for internal enynes (**d**), the alkyne rearrangement becomes a much more difficult process (**np-TS2Yd-3Yd** transition structure is located at 19.4 kcal mol^{-1} higher in free energy than separated reactants), and this makes the deactivation process by enynes of type **d** become significantly more energetically demanding than the productive *ene-then-yne* pathway ($\Delta G^{\ddagger}$ = 11.9 kcal mol^{-1}). Furthermore, the presence of methyl groups in the propargylic position also disfavors kinetically the **1Eb** + **b** reaction through the *yne-then-ene* pathway (**np-TS2Yb-3Yb** being located at 14.5 kcal mol^{-1} above separated reactants). Nevertheless, our results do not show that this process becomes more energetically demanding than the productive pathway, as should be expected from Fogg and co-workers' experiments.[27]

In summary, our calculations suggest that **1E** should be the major carbene in the reaction mixture, if **1E** and **1Y** reach equilibrium conditions. When nonsubstituted enynes are used **1E** would preferentially proceed through an *yne-then-ene* pathway that could favor a fast deactivation. Nevertheless, the presence of substituents in one of the unsaturated moieties of reacting enyne would significantly disfavor the nonproductive process.

As already mentioned in the Introduction, it is nowadays well accepted that Ru-based catalysts generally lead to the formation of the *exo* product.[29,32,34] Nevertheless, systematic experimental studies on the effect of the enyne substituents in the final product formation in RCEYM processes have shown that (i) nonsubstituted enynes are not good candidates for RCEYM reaction as the catalyst rapidly deactivates;[27] and (ii) the *endo* product can be obtained when the reacting enyne has an internal alkyne fragment.[29,32,34] The amount of *endo* product is usually low and only when the alkyne fragment is internal and the alkene fragment sterically hindered (geminal alkene) does the final product mixture present significant amounts of the *endo* isomer, comparable to those of the *exo* one. Our calculations reproduce reasonably well these general trends. First, they predict that the nonproductive pathways can be competitive with the catalytic cycles, especially when the reacting enyne is not substituted. This can be avoided at least in part by substituting the enyne. Moreover, results also suggest the preferential formation of the *exo* product for enynes with a terminal alkyne (**a**, **b**, and **c**). Furthermore, calculations show that for those species with an internal alkyne and 1,1-disubstituted alkene fragments (reactant **e**), good yields of the *endo* product should be expected, as observed experimentally. Unfortunately, if one considers the processes independently, our modeling approach seems to underestimate the viability of the *ene-then-yne* route as compared to experimental data. This is evidenced when analyzing the results obtained with enyne **d** and compared with similar systems available in the literature.[29] In this case, our data suggest the *ene-then-yne* pathway is slightly less favorable than the *yne-then-ene* mechanisms, and thus, since both *exo* and *endo* orientations are computed to have similar energetics, the RCEYM process of enyne **d** is predicted to lead to good amounts of both *exo* and *endo* products. The origin of this discrepancy can be due to the easy **1Y** to **1E** conversion, which reduces significantly the amount of **1Y** in the reaction mixture. As a consequence of this process, the *ene-then-yne* pathway could be favored because of the major presence of **1E**.

Overall, the good agreement found for reactants with a substituted alkene fragment encouraged us to analyze the role of other substituents rather than methyl groups in the alkyne fragment. Previously, results suggested that when the alkene fragment is substituted, the **1Y** to **1E** conversion is partially hindered, and thus, the reaction proceeds mainly through the *yne-then-ene* pathway. It is for this reason that we have only considered the reactivity starting from **1Y**, a situation that would be more representative of reactions taking place under the presence of ethene. To the best of our knowledge, the effect of including electron-donor and electron-withdrawing substituents has never been addressed from an experimental point of view.

Effect of Bulky, Electron-Donor and Electron-Withdrawing Groups in the *exo*-/*endo*- Selectivity. With the aim of determining the influence of other substituents rather than methyl groups in the vicinity of the alkyne moiety, we have considered the six additional systems (**h**−**k**) reported in Scheme 5. The selected species have been built as illustrative models that account for the effects of adding bulkier, electron-donor and electron-withdrawing groups in the key positions of the enyne and are not based on complexes existing in the literature. Note that all these reactants present a substituted alkene fragment that, according to our calculations, has an important role in hindering the *ene-then-yne* pathway as well as the formation of **1E**. Nevertheless, one should consider that the here presented results describe more properly reactions in the presence of ethene as we have explored only the *exo-yne-then-ene* and *endo-yne-then-ene* routes. In particular, we studied the

dx.doi.org/10.1021/cs300580g | *ACS Catal.* 2013, 3, 206−218

irreversible formation of ***exo*-3Y** and ***endo*-3Y**. The discussion will be done taking **e** as reference and analyzing the effect of including bulkier, stronger electron-donor and electron-withdrawing substituents in both terminal and propargylic positions. Table 4 summarizes the computed energies. The geometries of the optimized intermediates and transition structures can be found in the Supporting Information, Figures S17 and S22.

Table 4. Reaction Free Energies (ΔG) for the Alkyne Coordination Step (1Y + enyne → 2Y)[a] and Free Energy Barriers ($\Delta G^{\ddagger}$) Associated with the Global Alkyne Skeletal Reorganization (1Y + enyne → TS2Y-3Y)[a] of Enynes e−k[b]

	exo-yne-then-ene		*endo-yne-then-ene*	
reactant[c]	ΔG	$\Delta G^{\ddagger}$	ΔG	$\Delta G^{\ddagger}$
e	+2.9	+10.9	+6.6	+9.8
f	+5.6	+10.9	+5.7	+8.6
g	+5.3	+9.9	+7.2	+9.5
h	+2.6	+9.0	+3.6	+9.9
i	+5.0	+13.6	+4.5	+10.6
j	+0.4	+12.3	+3.1	+9.6
k	+1.6	+9.5	+1.7	+10.4

[a]See Scheme 4 for structures' definitions. [b]All values are in kcal mol^{-1}. [c]See Scheme 5 for reactants' definitions.

Substitution of terminal methyl by the bulkier and stronger electron-donor *ter*-butyl group (*t*Bu) (**f** in Scheme 5) has an effect on both the *exo*- and *endo-yne-then-ene* pathways. For the *exo* orientation, the alkyne coordination becomes more endergonic, which may have a role in retarding the reaction, but the alkyne skeletal reorganization barrier remains unaltered (Table 4). In contrast, the effect of this substitution in the *endo-yne-then-ene* route is somewhat different: the coordination is also disfavored, but the presence of the *t*Bu group slightly facilitates the alkyne skeletal reorganization with respect to the same process with enyne **e**. The relative energy of ***endo*-TS2Yf-3Yf** with respect to separated reactants decreases by 1.2 kcal mol^{-1}. Therefore, the *endo-yne-then-ene* route seems to be slightly easier than the *exo-yne-then-ene* one. A similar substitution at the propargylic position (enyne **g** in Scheme 5) has essentially the opposite effect. The *endo-yne-then-ene* route is almost unaltered, and the *exo-yne-then-ene* one becomes easier by 1.0 kcal mol^{-1} with respect to that with enyne **e**.

On the other hand, the effect of bulkier but electron-withdrawing groups have also been considered by replacing the terminal and propargylic hydrogens by fluorine atoms (**h** and **i** in Scheme 5). With this substitution, one would expect effects similar to those observed when adding methyl groups to **e** if only steric effects are dominant. The addition of electron-withdrawing groups increases, in general, the energy barrier of the two pathways; the main exception is enyne **h**. Nevertheless, this effect is strongly influenced by the substituent position, and thus, it may tune the *exo*-/*endo*- selectivity. The substitution of the terminal CH_3 by a CF_3 has almost no effect on the *endo-yne-then-ene* route, but it decreases significantly the energy barrier of the *exo-yne-then-ene* pathway by almost 2 kcal mol^{-1}. Therefore, the reaction through the *exo* route is computed to be lower in free energy. This is the opposite effect to what was computed for the addition of the *t*Bu group (**f**) (Table 4), and thus, it suggests that effects other than the sterics play a role in the product selectivity. Moreover, when fluorine atoms are added at the propargylic position (**i**), both the *exo*- and *endo*- routes are disfavored with respect to reactant **e**. Nevertheless, the effect is larger for the *exo-yne-then-ene* route, and thus, the *endo* orientation becomes favored with respect to *exo-yne-then-ene* pathway, especially compared to **e**. This situation contrasts with the values obtained when the substituents in the propargylic position are methyls, suggesting again that the effect is not only steric.

In summary, the energetic effects induced by the presence of fluorine groups are essentially of opposite sign to those described by the addition of methyl groups in the same positions. Therefore, the here presented data suggest that effects other than sterics are important. An additional proof for this interpretation arises from the results obtained for enyne **j**, with cyanide groups instead of fluorine atoms in the propargylic position. The values computed with reactant **j** show the same trends as those of enyne **i**, reinforcing the idea that the electronic nature of the substituents would be relevant in determining the major product of the catalytic reaction.

The energy difference within all explored pathways is small, the number of examples is limited, and several factors contribute to the final energetics (reactant−catalyst interaction, entropic contribution, solvation, dispersion forces, etc.). Thus, it is not easy to identify the origin of the subtle differences. Nevertheless, two main conclusions seem to arise from the here performed calculations: (i) substituted alkene moieties prevent the **1Y** to **1E** interconvertion and react preferentially through an *yne-then-ene* mechanism, thus allowing the potential formation of the two products; and (ii) the preference for the formation of the *exo* or *endo* product depends on the substituents in the nearby of the alkyne fragment. In this way, terminal alkyne fragments could proceed preferentially through an *exo-yne-then-ene* pathway when the alkene moiety is substituted. It is remarkable that all considered terminal alkyne fragments prefer to proceed through an *exo-yne-then-ene* orientation, regardless of the nature of the substituents in the propargylic position (electron-donor or electron-withdrawing). This correlates with a larger negative charge on the terminal carbon atom of the alkyne fragment (Supporting Information, Table S23). On the other hand, for enynes having internal alkyne fragments, the atomic charges of the two carbons of the alkyne are much more similar, and the two pathways become closer in energy. In these cases, both the sterics and the electronic properties of the two carbons of the alkyne fragment are similar and, thus, react similarly. Overall, the *exo*/*endo-yne-then-ene* selectivity seems to be at least in part driven by factors other rather than the sterics.

CONCLUSIONS

The influence of enyne substituents in the feasibility of the three proposed pathways (*ene-then-yne*, *exo-yne-then-ene*, and *endo-yne-then-ene*) for the Ring Closing Enyne Metathesis has been analyzed. For this, the energetics of the three pathways have been computed for a series of 11 different enyne models containing the 1-allyloxyprop-2-yne skeleton with substituents at the alkyne terminal position, propargylic carbon, and alkene fragment. In addition, two nonproductive pathways arising from the interaction of the unsaturated fragment that does not lead to the catalytic cycle with the two active carbenes have been considered. These two processes interconvert the methylidene carbene with **1E** in one case and could lead to catalyst deactivation in the second. The here reported study allows a better understanding of the available experimental data and outlines which kind of substituted enynes could eventually lead to the major formation of the *endo* product. First of all, the

dx.doi.org/10.1021/cs300580g | *ACS Catal.* 2013, 3, 206−218

addition of substituents in the alkene and alkyne fragments disfavors the nonproductive pathways. Moreover, enynes with substituted alkene fragments preferentially proceed through an *yne-then-ene* route as the presence of a methyl substituent in the alkene fragment is sufficient to disfavor the *ene-then-yne* route. In these cases, if the alkyne fragment has no substituents, the most favorable pathway is the *exo-yne-then-ene* route. Nevertheless, for internal alkyne fragments, the two processes become competitive, and the preferred pathway does not seem to be controlled uniquely by the steric requirements of the substituents. Note that in these last cases, the atomic charges of the two carbons of the alkyne fragment, which are significantly different in the terminal alkynes, become similar, and thus, for internal alkynes, the two carbons present similar sterics and electronics.

■ ASSOCIATED CONTENT

Supporting Information

Table S1 reporting the B3LYP/BSC free energies with respect to separated reactants of the key ***exo/endo*-TS2Y-3Y** transition structures. Figure S1 depicting the B3LYP/BSC optimized structures of the key ***exo/endo*-TS2Y-3Y** transition structures. Figure S2 to S22 showing the B3LYP/BSA optimized structures of all intermediates and transition states reported in the manuscript. Full list of Cartesian coordinates of all stationary points with their absolute energies, gas phase free energies, and solvation free energies. This material is available free of charge via the Internet at http://pubs.acs.org.

■ AUTHOR INFORMATION

Corresponding Author

*E-mail: xavi@klingon.uab.es.

Notes

The authors declare no competing financial interest.

■ ACKNOWLEDGMENTS

We acknowledge financial support from MICINN (CTQ2011-24847/BQU) and the Generalitat de Catalunya (SGR2009-638). F.N.Z. wishes to thank to Universitat Autònoma de Barcelona for his Ph.D. PIF scholarship. X.S.M. thanks the Spanish MEC/MICINN for his Ramón y Cajal fellowship. M.S. gratefully acknowledges support through 2011 ICREA Academia award.

■ REFERENCES

(1) Katz, T. J.; Sivavec, T. M. *J. Am. Chem. Soc.* **1985**, *107*, 737−738.
(2) Kinoshita, A.; Mori, M. *Synlett* **1994**, 1020−1022.
(3) Diver, S. T.; Giessert, A. J. *Chem. Rev.* **2004**, *104*, 1317−1382.
(4) Calderon, N.; Chen, H. Y.; Scott, K. W. *Tetrahedron Lett.* **1967**, *8*, 3327−3330.
(5) Fürstner, A. *Angew. Chem., Int. Ed.* **2000**, *39*, 3013−3043.
(6) Chauvin, Y. *Angew. Chem., Int. Ed.* **2006**, *45*, 3740−3747.
(7) Schrock, R. R. *Angew. Chem., Int. Ed.* **2006**, *45*, 3748−3759.
(8) Grubbs, R. H. *Angew. Chem., Int. Ed.* **2006**, *45*, 3760−3765.
(9) Deshmukh, P. H.; Blechert, S. *Dalton Trans.* **2007**, 2479−2491.
(10) Mori, M.; Sakakibara, N.; Kinoshita, A. *J. Org. Chem.* **1998**, *63*, 6082−6083.
(11) Deiters, A.; Martin, S. F. *Chem. Rev.* **2004**, *104*, 2199−2238.
(12) Nicolaou, K. C.; Bulger, P. G.; Sarlah, D. *Angew. Chem., Int. Ed.* **2005**, *44*, 4490−4527.
(13) Villar, H.; Frings, M.; Bolm, C. *Chem. Soc. Rev.* **2007**, *36*, 55−66.
(14) Mori, M. *Adv. Synth. Catal.* **2007**, *349*, 121−135.
(15) Lloyd-Jones, G. C. *Org. Biomol. Chem.* **2003**, *1*, 215−236.
(16) Singh, R.; Schrock, R. R.; Müller, P.; Hoveyda, A. H. *J. Am. Chem. Soc.* **2007**, *129*, 12654−12655.
(17) Lee, Y. J.; Schrock, R. R.; Hoveyda, A. H. *J. Am. Chem. Soc.* **2009**, *131*, 10652−10661.
(18) Zhao, Y.; Hoveyda, A. H.; Schrock, R. R. *Org. Lett.* **2011**, *13*, 784−787.
(19) Diver, S. T. *Coord. Chem. Rev.* **2007**, *251*, 671−701.
(20) Elias, X.; Pleixats, R.; Wong Chi Man, M. *Tetrahedron* **2008**, *64*, 6770−6781.
(21) Sanford, M. S.; Love, J. A.; Grubbs, R. H. *J. Am. Chem. Soc.* **2001**, *123*, 6543−6554.
(22) Love, J. A.; Morgan, J. P.; Trnka, T. M.; Grubbs, R. H. *Angew. Chem., Int. Ed.* **2002**, *41*, 4035−4037.
(23) Love, J. A.; Sanford, M. S.; Day, M. W.; Grubbs, R. H. *J. Am. Chem. Soc.* **2003**, *125*, 10103−10109.
(24) Kingsbury, J. S.; Hoveyda, A. H. *J. Am. Chem. Soc.* **2005**, *127*, 4510−4517.
(25) Ashworth, I. W.; Hillier, I. H.; Nelson, D. J.; Percy, J. M.; Vincent, M. A. *Chem. Commun.* **2011**, *47*, 5428−5430.
(26) Thiel, V.; Hendann, M.; Wannowius, K. J.; Plenio, H. *J. Am. Chem. Soc.* **2012**, *134*, 1104−1114.
(27) Grotevendt, A. G. D.; Lummiss, J. A. M.; Mastronardi, M. L.; Fogg, D. E. *J. Am. Chem. Soc.* **2011**, *133*, 15918−15921.
(28) Hoye, T. R.; Donaldson, S. M.; Vos, T. J. *Org. Lett.* **1999**, *1*, 277−279.
(29) Kitamura, T.; Sato, Y.; Mori, M. *Adv. Synth. Catal.* **2002**, *344*, 678−693.
(30) Lloyd-Jones, G. C.; Margue, R. G.; de Vries, J. G. *Angew. Chem., Int. Ed.* **2005**, *44*, 7442−7447.
(31) Hansen, E. C.; Lee, D. *Acc. Chem. Res.* **2006**, *39*, 509−519.
(32) Sashuk, V.; Grela, K. *J. Mol. Catal. A: Chem.* **2006**, *257*, 59−66.
(33) Kim, K. H.; Ok, T.; Lee, K.; Lee, H. S.; Chang, K. T.; Ihee, H.; Sohn, J. H. *J. Am. Chem. Soc.* **2010**, *132*, 12027−12033.
(34) Kitamura, T.; Sato, Y.; Mori, M. *Chem. Commun.* **2001**, 1258−1259.
(35) Nuñez-Zarur, F.; Solans-Monfort, X.; Rodríguez-Santiago, L.; Pleixats, R.; Sodupe, M. *Chem.—Eur. J.* **2011**, *17*, 7506−7520.
(36) Dieltiens, N.; Moonen, K.; Stevens, C. V. *Chem.—Eur. J.* **2007**, *13*, 203−214.
(37) Clavier, H.; Correa, A.; Escudero-Adan, E. C.; Benet-Buchholz, J.; Cavallo, L.; Nolan, S. P. *Chem.—Eur. J.* **2009**, *15*, 10244−10254.
(38) Adlhart, C.; Chen, P. *Angew. Chem., Int. Ed.* **2002**, *41*, 4484−4487.
(39) Cavallo, L. *J. Am. Chem. Soc.* **2002**, *124*, 8965−8973.
(40) Vyboishchikov, S. E.; Bühl, M.; Thiel, W. *Chem.—Eur. J.* **2002**, *8*, 3962−3975.
(41) Adlhart, C.; Chen, P. *J. Am. Chem. Soc.* **2004**, *126*, 3496−3510.
(42) Suresh, C. H.; Koga, N. *Organometallics* **2004**, *23*, 76−80.
(43) Vyboishchikov, S. E.; Thiel, W. *Chem.—Eur. J.* **2005**, *11*, 3921−3935.
(44) Straub, B. F. *Angew. Chem., Int. Ed.* **2005**, *44*, 5974−5978.
(45) Solans-Monfort, X.; Clot, E.; Copéret, C.; Eisenstein, O. *J. Am. Chem. Soc.* **2005**, *127*, 14015−14025.
(46) Correa, A.; Cavallo, L. *J. Am. Chem. Soc.* **2006**, *128*, 13352−13353.
(47) Zhao, Y.; Truhlar, D. G. *Org. Lett.* **2007**, *9*, 1967−1970.
(48) Straub, B. F. *Adv. Synth. Catal.* **2007**, *349*, 204−214.
(49) Poater, A.; Solans-Monfort, X.; Clot, E.; Copéret, C.; Eisenstein, O. *J. Am. Chem. Soc.* **2007**, *129*, 8207−8216.
(50) Benitez, D.; Tkatchouk, E.; Goddard, W. A. *Chem. Commun.* **2008**, 6194−6196.
(51) Mathew, J.; Koga, N.; Suresh, C. H. *Organometallics* **2008**, *27*, 4666−4670.
(52) Diesendruck, C. E.; Tzur, E.; Ben-Asuly, A.; Goldberg, I.; Straub, B. F.; Lemcoff, N. G. *Inorg. Chem.* **2009**, *48*, 10819−10825.
(53) Stewart, I. C.; Benitez, D.; O'Leary, D. J.; Tkatchouk, E.; Day, M. W.; Goddard, W. A.; Grubbs, R. H. *J. Am. Chem. Soc.* **2009**, *131*, 1931−1938.

(54) Ragone, F.; Poater, A.; Cavallo, L. *J. Am. Chem. Soc.* **2010**, *132*, 4249−4258.
(55) Poater, A.; Ragone, F.; Correa, A.; Szadkowska, A.; Barbasiewicz, M.; Grela, K.; Cavallo, L. *Chem.—Eur. J.* **2010**, *16*, 14354−14364.
(56) Solans-Monfort, X.; Pleixats, R.; Sodupe, M. *Chem.—Eur. J.* **2010**, *16*, 7331−7343.
(57) Solans-Monfort, X.; Copéret, C.; Eisenstein, O. *J. Am. Chem. Soc.* **2010**, *132*, 7750−7757.
(58) Herbert, M. B.; Lan, Y.; Keitz, B. K.; Liu, P.; Endo, K.; Day, M. W.; Houk, K. N.; Grubbs, R. H. *J. Am. Chem. Soc.* **2012**, *134*, 7861−7866.
(59) Liu, P.; Xu, X. F.; Dong, X. F.; Keitz, B. K.; Herbert, M. B.; Grubbs, R. H.; Houk, K. N. *J. Am. Chem. Soc.* **2012**, *134*, 1464−1467.
(60) Lippstreu, J. J.; Straub, B. F. *J. Am. Chem. Soc.* **2005**, *127*, 7444−7457.
(61) Garcia-Fandino, R.; Castedo, L.; Granja, J. R.; Cardenas, D. J. *Dalton Trans.* **2007**, 2925−2934.
(62) Elias, X.; Pleixats, R.; Wong Chi Man, M.; Moreau, J. J. E. *Adv. Synth. Catal.* **2007**, *349*, 1701−1713.
(63) Nuñez-Zarur, F.; Solans-Monfort, X.; Rodríguez-Santiago, L.; Sodupe, M. *Organometallics* **2012**, *31*, 4203−4215.
(64) Becke, A. D. *J. Chem. Phys.* **1993**, *98*, 5648−5652.
(65) Lee, C. T.; Yang, W. T.; Parr, R. G. *Phys. Rev. B* **1988**, *37*, 785−789.
(66) Frisch, M. J.; Trucks, G. W.; Schlegel, H. B.; Scuseria, G. E.; Robb, M. A.; Cheeseman, J. R.; Montgomery, J. A.; Jr., T., V.; Kudin, K. N.; Burant, J. C.; Millam, J. M.; Iyengar, S. S.; Tomasi, J.; Barone, V.; Mennucci, B.; Cossi, M.; Scalmani, G.; Rega, N.; Petersson, G. A.; Nakatsuji, H.; Hada, M.; Ehara, M.; Toyota, K.; Fukuda, R.; Hasegawa, J.; Ishida, M.; Nakajima, T.; Honda, Y.; Kitao, O.; Nakai, H.; Klene, M.; Li, X.; Knox, J. E.; Hratchian, H. P.; Cross, J. B.; Adamo, C.; Jaramillo, J.; Gomperts, R.; Stratmann, R. E.; Yazyev, O.; Austin, A. J.; Cammi, R.; Pomelli, C.; Ochterski, J. W.; Ayala, P. Y.; Morokuma, K.; Voth, G. A.; Salvador, P.; Dannenberg, J. J.; Zakrzewski, V. G.; Dapprich, S.; Daniels, A. D.; Strain, M. C.; Farkas, O.; Malick, D. K.; Rabuck, A. D.; Raghavachari, K.; Foresman, J. B.; Ortiz, J. V.; Cui, Q.; Baboul, A. G.; Clifford, S.; ; Cioslowski, J.; Stefanov, B. B.; Liu, G.; Liashenko, A.; Piskorz, P.; Komaromi, I.; Martin, R. L.; Fox, D. J.; Keith, T.; Al-Laham, M. A.; Peng, C. Y.; Nanayakkara, A.; Challacombe, M.; Gill, P. M. W.; Johnson, B.; Chen, W.; Wong, M. W.; Gonzalez, C.; Pople, J. A. *Gaussian 03*, Rev. B.04; Gaussian Inc.: Pittsburgh, PA, 2003.
(67) Küchle, W.; Dolg, M.; Stoll, H.; Preuss, H. *Mol. Phys.* **1991**, *74*, 1245−1263.
(68) Ehlers, A. W.; Böhme, M.; Dapprich, S.; Gobbi, A.; Höllwarth, A.; Jonas, V.; Köhler, K. F.; Stegmann, R.; Veldkamp, A.; Frenking, G. *Chem. Phys. Lett.* **1993**, *208*, 111−114.
(69) Francl, M. M.; Pietro, W. J.; Hehre, W. J.; Binkley, J. S.; Gordon, M. S.; Defrees, D. J.; Pople, J. A. *J. Chem. Phys.* **1982**, *77*, 3654−3665.
(70) Hehre, W. J.; Ditchfield, R.; Pople, J. A. *J. Chem. Phys.* **1972**, *56*, 2257−2261.
(71) Hariharan, P. C.; Pople, J. A. *Theor. Chim. Acta* **1973**, *28*, 213−222.
(72) Miertus, S.; Scrocco, E.; Tomasi, J. *Chem. Phys.* **1981**, *55*, 117−129.
(73) Barone, V.; Cossi, M. *J. Phys. Chem. A* **1998**, *102*, 1995−2001.
(74) Cossi, M.; Rega, N.; Scalmani, G.; Barone, V. *J. Comput. Chem.* **2003**, *24*, 669−681.
(75) Barone, V.; Cossi, M.; Tomasi, J. *J. Chem. Phys.* **1997**, *107*, 3210−3221.
(76) Sliwa, P.; Handzlik, J. *Chem. Phys. Lett.* **2010**, *493*, 273−278.
(77) Minenkov, Y.; Occhipinti, G.; Jensen, V. R. *J. Phys. Chem. A* **2009**, *113*, 11833−11844.
(78) Grimme, S. *J. Comput. Chem.* **2004**, *25*, 1463−1473.
(79) Grimme, S. *J. Comput. Chem.* **2006**, *27*, 1787−1799.
(80) Ugliengo, P.; Viterbo, D.; Chiari, G. *Z. Kristallogr.* **1993**, *207*, 9.
(81) Ackermann, L.; Fürstner, A.; Weskamp, T.; Kohl, F. J.; Herrmann, W. A. *Tetrahedron Lett.* **1999**, *40*, 4787−4790.
(82) Michrowska, A.; Bujok, R.; Harutyunyan, S.; Sashuk, V.; Dolgonos, G.; Grela, K. *J. Am. Chem. Soc.* **2004**, *126*, 9318−9325.
(83) Stewart, I. C.; Ung, T.; Pletnev, A. A.; Berlin, J. M.; Grubbs, R. H.; Schrodi, Y. *Org. Lett.* **2007**, *9*, 1589−1592.
(84) Berlin, J. M.; Campbell, K.; Ritter, T.; Funk, T. W.; Chlenov, A.; Grubbs, R. H. *Org. Lett.* **2007**, *9*, 1339−1342.
(85) Kirkland, T. A.; Grubbs, R. H. *J. Org. Chem.* **1997**, *62*, 7310−7318.
(86) Costabile, C.; Mariconda, A.; Cavallo, L.; Longo, P.; Bertolasi, V.; Ragone, F.; Grisi, F. *Chem.—Eur. J.* **2011**, *17*, 8618−8629.